The Use of Matched Four-Port Filters to Realize Switched Multiplexers Having Low Amplitude and Group Delay Ripple

CHRISTOPHER I. MOBBS, MEMBER, IEEE

Abstract—A design method for channelizers and multiplexers is presented with particular emphasis on simplicity of design and alignment. By using two recombining multiplexers, one for the odd-numbered channels and one for the even-numbered channels, a high-performance switched multiplexer may be realized. The key to this performance is a multiplexer based on channel filters with integral hybrids which is designed to be matched in both passband and stopband.

The design criteria for such devices are presented for filters having finite Q structures. An eight-channel switched multiplexer in S-band is described, with experimental results in close agreement with theory.

I. Introduction

SWITCHED MULTIPLEXERS are receiving increasing attention for use in modern sophisticated ECM and ESM systems. By providing a degree of adaptive filtering in the RF portion of a system, performance may be enhanced and digital signal sorting may be simplified. It is important, however, that the overall performance of the system not be degraded as a result of signal distortion due to poor amplitude and phase characteristics.

Whereas a switched filterbank has only $N+1$ possible states for an N-channel device (allowing for all channels to be switched off), the switched multiplexer has 2^N states for the same number of channels. The performance of the switched filterbank (Fig. 1) is entirely determined by the characteristics of the switches and individual channel filters. As long as the filters and switches are designed to operate in a 50-Ω system, the performance of the complete unit is easily characterized.

The general form of an N-channel switched multiplexer is shown in Fig. 2 and is considerably more complex. Not only is the individual channel performance important, but channel interactions in any combination must be accounted for in the design of any device.

Due to the number of possible switching states for a complex device (over 60 000 for a typical 16-channel design), not only must the design be consistent with all these states, but the device must be capable of being aligned without need to select the majority of possible configurations.

Manuscript received April 14, 1987; revised August 4, 1987.

The author is with the Future Products Group of Filtronic Components Ltd., Charlestown, Shipley, W. Yorks. BD17 7SW, U.K.

IEEE Log Number 8717101.

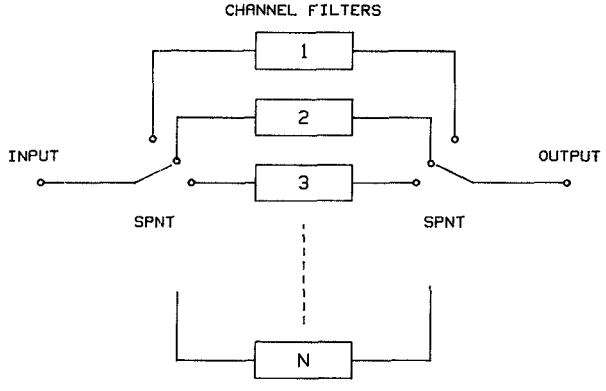

Fig. 1. Typical switched filterbank.

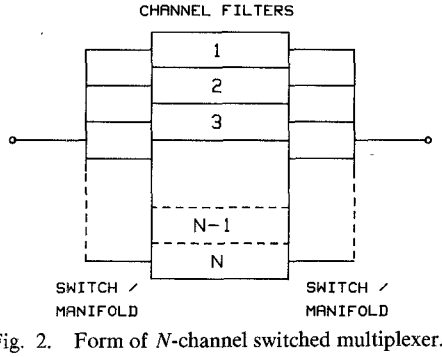

Fig. 2. Form of N-channel switched multiplexer.

One of the most logical ways to satisfy the above conditions is to make the multiplexer have a broad-band input and output match under all switching conditions, and to simplify the manifold and switching circuits by switching the channel filters internally. This switching technique is easily accomplished by using p-i-n diodes or switching FET's on the central resonators of each channel filter.

Conventional lossless manifold multiplexer designs depend on accounting for all the interactions between the channel filters and become very involved for large numbers of channels. The use of "lossy" manifold techniques [1], where a deliberate mismatch is introduced at the input of each channel filter, reduces channel interactions but still does not allow simple switching of channel filters without degrading adjacent channel performance.

0018-9480/87/1200-1183$01.00

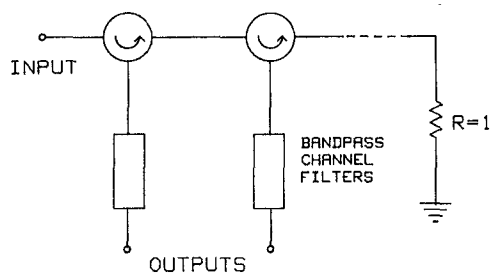

Fig. 3. Multiplexer using circulators.

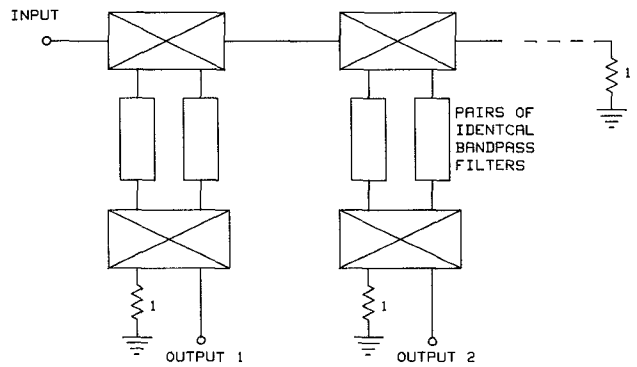

Fig. 4. Multiplexer using 3-dB quadrature hybrids.

A well-established technique for the design of bandpass channel multiplexers is shown in Fig. 3. The use of circulators for each channel filter eliminates channel interactions, and signals in the stopbands of all channels are dissipated in the terminating resistor at the end of the manifold. The major disadvantage resulting from the use of this method is the weight and bulk of the circulators and the considerable insertion loss of each circulator. This results in increased insertion loss in channels which are connected near the terminated end of the manifold. This effect can be minimized by deliberately using a lower Q structure for the earlier channels, but this results in a general increase in insertion loss and poor amplitude flatness for the low-Q filters.

A similar effect to that obtained by the use of circulators can be achieved by the structure of Fig. 4. The use of 3-dB quadrature hybrids results in the number of channel filters being doubled but has the advantage over circulators that the weight penalty incurred need not be as great and the insertion loss of the hybrids may be significantly lower than the circulators. To achieve good performance, however, the pairs of nominally identical filters in each channel must be well matched. This condition may be satisfied by integrating the manifold, hybrids, and channel filters on to a single MIC substrate.

This hybrid multiplexer approach was therefore used for the development of a switched multiplexer design.

II. Integrated Hybrid/Filter Design

The form of a single channel filter matched at all four ports is shown in Fig. 5. It is only necessary for the hybrid to function as a true hybrid over the band of the associated channel filter. Provided the hybrid has all pass characteristics between parts 1 and 2 (as shown in Fig. 5), the hybrid will perform the required function.

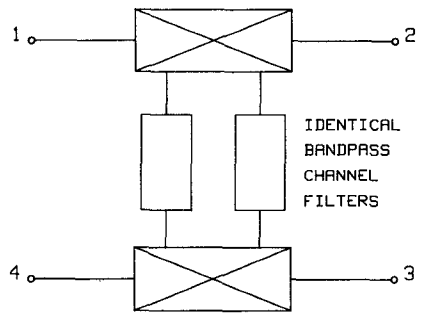

Fig. 5. Single hybrid channel.

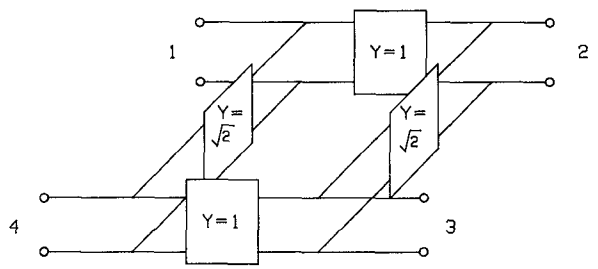

Fig. 6. Impedance inverter hybrid.

The basic form of a 3-dB branch line hybrid is shown in Fig. 6. This general form has infinite bandwidth if frequency-independent impedance inverters could be realized. An identical analysis method can be applied to both a single hybrid and the complete hybrid/filter assembly. As both networks have two orthogonal planes of symmetry, we may proceed as follows. For a symmetrical two-port, Bartlett's bisection theorem can be used to give the identities used by Rhodes [2]:

$$S_{11}(p) = \frac{1 - Y_e(p) \cdot Y_o(p)}{(1 + Y_e(p))(1 + Y_o(p))} \tag{1}$$

and

$$S_{12}(p) = \frac{Y_e(p) - Y_o(p)}{(1 + Y_e(p))(1 + Y_o(p))} \tag{2}$$

where $Y_e(p)$ and $Y_o(p)$ are the input admittances of the network when an open circuit or short circuit, respectively, is placed down the plane of symmetry.

In a similar manner, we may produce the following for a four-port network:

$$R_e(p) = \frac{1 - Y_{ee}(p) \cdot Y_{eo}(p)}{(1 + Y_{ee}(p))(1 + Y_{eo}(p))} \tag{3}$$

$$T_e(p) = \frac{Y_{ee}(p) - Y_{eo}(p)}{(1 + Y_{ee}(p))(1 + Y_{eo}(p))} \tag{4}$$

$$R_o(p) = \frac{1 - Y_{oe}(p) \cdot Y_{oo}(p)}{(1 + Y_{oe}(p))(1 + Y_{oo}(p))} \tag{5}$$

$$T_o(p) = \frac{Y_{oe}(p) - Y_{oo}(p)}{(1 + Y_{oe}(p))(1 + Y_{oo}(p))}. \tag{6}$$

These may be considered as the even- and odd-mode reflection and transmission coefficients. The S parameters of the complete four-port may then be obtained by superposition. These are

$$S_{11}(p)=\frac{1}{2}(R_e(p)+R_o(p))$$

$$S_{12}(p)=\frac{1}{2}(T_e(p)+T_o(p))$$

$$S_{14}(p)=\frac{1}{2}(R_e(p)-R_o(p))$$

$$S_{13}(p)=\frac{1}{2}(T_e(p)-T_o(p)). \tag{7}$$

For the simple impedance inverter hybrid, equations (7) give

$$S_{11}=0 \qquad S_{12}=0$$

$$S_{14}=\frac{-j}{\sqrt{2}} \qquad S_{19}=\frac{1}{\sqrt{2}}. \tag{8}$$

This shows power is split equally between ports 3 and 4 with a 90° phase difference between them.

A hybrid consisting of quarter-wave transmission lines will give identical performance to the ideal inverter hybrid at band center and has a 10–15 percent usable bandwidth. As most switched multiplexers are required to operate over a bandwidth in excess of one octave, it is necessary to use a structure which has a broad-band characteristic for which $|S_{12}| \approx 1$. This is possible by integrating the hybrid into the first elements of each bandpass filter as follows.

An impedance inverter (in cascade with a $1:-1$ transformer) may be realized by a Π of inductors or capacitors as shown in Fig. 7. These networks have characteristic admittance $1/\omega L$ and ωC, respectively. It is possible to scale the admittance of any port in the hybrid network by a factor k. This has the effect of scaling the adjacent inverters by a factor $\sqrt{k}$.

Using these properties, the network of Fig. 8 may be derived. The elements L_0 and C_0 form a circuit resonant at ω_0, which is the band-center frequency of the hybrid. The negative shunt capacitors and inductors from the inverters are absorbed into the resonators to give the values shown in Fig. 8, where $L_1=(L\cdot L_0)/(L-L_0)$. The impedance inverter between ports 1 and 2 remains as a transmission line of unity admittance. If the impedance at ports 3 and 4 is large, the capacitors required to produce the inverters (of admittance $1/\sqrt{(2k)}$) will be small. Hence the negative shunt capacitor at ports 1 and 2 may be realized by increasing the impedance of the transmission line for a very short distance on either side of the capacitor junction.

This network has bandpass properties at ports 3 and 4, and the transmission between ports 1 and 2 is limited by the effect of the coupling capacitors, C, which, combined with the added series inductance to compensate for the negative shunt capacitors, forms a low-pass filter. This low-pass must be made to have a cutoff frequency above the highest frequency of operation of the entire multiplexer.

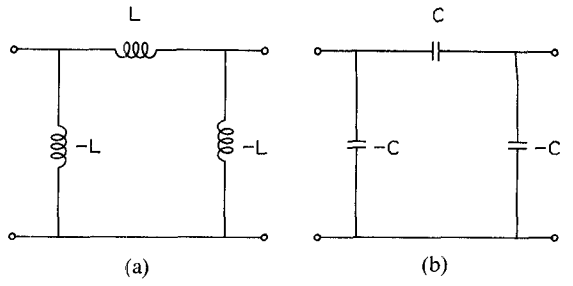

Fig. 7. Pi section impedance inverters.

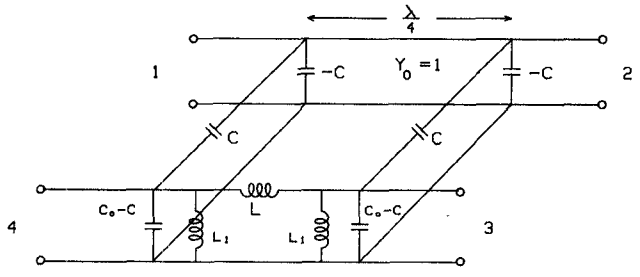

Fig. 8. Lumped form of hybrid.

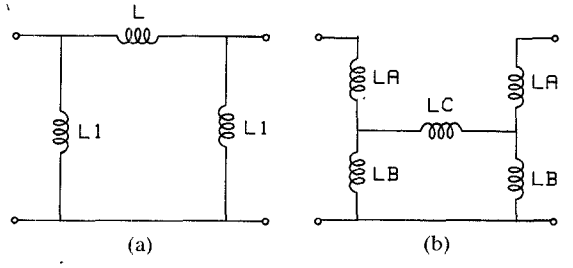

Fig. 9. Equivalent inductor networks for hybrid coupling.

The network of Fig. 8 has realizable values for all elements with the exception of the coupling inductor L. For narrow bandwidths, this inductor becomes very large. This problem is easily overcome by using the circuit equivalence of Fig. 9. In the limiting case where $L_A=0$, the simple identities

$$L_A=\frac{L\cdot L_1}{L+2L_1} \tag{9}$$

and

$$L_B=L_1-L_A$$

may be derived by considering the even- and odd-mode admittances of each network.

The design of the overall hybrid filter network is therefore quite simple. The bandpass channel filters, which have small percentage bandwidths, are designed using a shunt resonator, inverter coupled prototype filter as shown in Fig. 10. The filter is symmetrical (i.e., $L_n=L_1$ and $C_n=C_1$, etc.) and is not scaled in impedance, as is usual for a narrow-band filter, so as to maintain the direct coupling into the first resonator. An impedance scaling factor, $1/k$, is chosen to give realizable internal impedance levels for

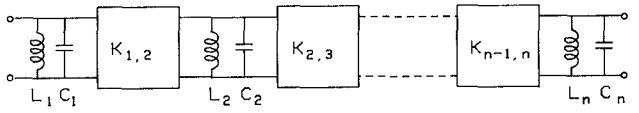

Fig. 10. Inverter coupled bandpass filter.

the bandpass channels. Hence the value of the capacitors, C, of Fig. 8 may be calculated using the fact that

$$\omega_0 C = \sqrt{(2k)}. \tag{10}$$

The coupling inductor L satisfies the equation

$$1/(\omega_0 L) = k. \tag{11}$$

Using the identities of (9), a direct tap between the first shunt inductor of each channel filter may be used to realize this element.

As an alternative to adding series inductance in the line in the region of the coupling capacitors, the length of line between the two arms of the hybrid may be modified. This length is nominally $\lambda/4$ at the band-center frequency of the associated channel filter. The negative shunt capacitor modifies the imaginary part of the even- and odd-mode admittances at ports 1 and 2. These admittances are of the form

$$\mathrm{Im}(Y_e) = Y_e' - \omega_0 C + \tan\theta \tag{12}$$

$$\mathrm{Im}(Y_o) = Y_o' - \omega_0 C - \cot\theta. \tag{13}$$

Normally θ would be 45°, i.e., $\tan\theta = \cot\theta = 1$, but let us choose a new angle θ such that

$$\tan\theta = 1 - \omega_0 C$$

i.e.,

$$\theta_1 = \tan^{-1}(1 - \omega_0 C). \tag{14}$$

Applying a similar procedure to (13) gives

$$\theta_2 = \tan^{-1}\left[\frac{1}{1+\omega_0 C}\right] \tag{15}$$

for small $\omega_0 C$, therefore, $\theta_1 \approx \theta_2$. A typical filter would be scaled in internal impedance by a factor of 50. Hence $\omega_0 C = 0.2$ from (10) and $\theta \approx 39°$. The line length between ports 1 and 2 is therefore 78°. This results in a good input VSWR in the region of the filter passband and is applicable to channel filters of narrow or moderate bandwidths.

III. Channel Switching

The four-port hybrid filter lends itself well to simple switching methods. The properties of the 90° hybrid are such that if two equal reactive mismatches are placed at ports 3 and 4, then perfect transmission occurs from port 1 to port 2. This reactive mismatch may be in the form of a p-i-n diode or switching FET on the second and $(n-1)$th resonators in each filter. The match at all four ports of the balanced filter will be preserved but there will be no transmission from input to output assuming the diodes are perfect. Signals applied to the input of the device are therefore dissipated in the load resistor at the end of the input manifold rather than passing through the device.

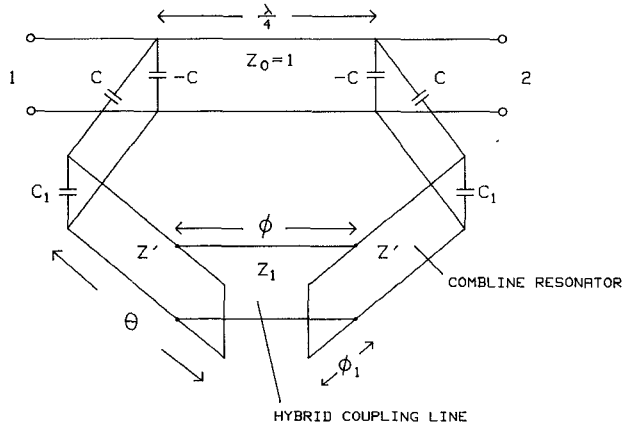

Fig. 11. Distributed form of hybrid.

Although adequate isolation may be achieved using switches on just two filter resonators, improved isolation can be obtained by placing p-i-n diodes on some of the central resonators of each channel filter.

IV. Distributed Channel Filters

The design procedure described so far deals with a lumped element realization for the channel filters. Although lumped component techniques may be applied to devices operating at frequencies up to 10 GHz and beyond, their use in complex multiplexer circuits could give rise to severe difficulties in terms of reproducibility and tracking between the two nominally identical arms of each channel filter. It is desirable therefore to utilize a printed circuit, distributed realization for the channel filters.

The most convenient form of narrow-band channel filter which is realizable in printed circuit form (strip line or suspended substrate strip line) is the combline filter [3]. Parallel coupled transmission lines may be printed on the substrate to form the coupled short-circuit stubs, the lumped capacitors being realized by parallel-plate coupling through the dielectric or by reducing the ground plane spacing over the ends of each resonator.

The design of the internal elements of each filter follows standard design procedures, and the physical dimensions may be derived from Getsinger's graphs [4]. The form of the distributed narrow-band hybrid is shown in Fig. 11, where the through line between ports 1 and 2 is unchanged from the lumped case, and the coupling capacitors, C_A, are derived as before after choosing an admittance scaling factor to give realizable line impedances for the combline resonators. In a similar manner C_1 is calculated as

$$C_1 = C_r - C \tag{16}$$

where

$$C_r = \frac{1}{\omega_0 Z \tan\theta} \tag{17}$$

ω_0 being the band-center angular frequency and Z the characteristic impedance of the combline resonator.

The required coupling between the combline resonators may be evaluated as follows. Choosing a value for the

impedance of the coupling line, Z, ϕ_1 (the tap point) may be evaluated for different values of ϕ (the length of the coupling line). A new resonator characteristic admittance, Z', is required to account for the effect of the shunt arms of the coupling inverter. For an admittance scaling factor k, we may write for the lumped element network of Fig. 9

$$Y_e - Y_o = j(2k) \tag{18}$$

using the identity of (11). Now for the network of Fig. 11,

$$Y_{e,o} = Y' \frac{Y_2 + jY' \tan(\theta - \phi_1)}{Y' + jY_2 \tan(\theta - \phi_1)} \tag{19}$$

where

$$Y_2 = j\left[Y_1 \tan(\phi/2) - Y' \cot \phi_1\right] \tag{20}$$

for the even mode, and

$$Y_2 = j\left[-Y_1 \cot(\phi/2) - Y' \cot \phi_1\right] \tag{21}$$

for the odd mode.

The additional design requirement is that the characteristic admittance of the resonators be such that the overall network have the correct resonant frequency and impedance. Now assuming the coupling admittance is much less than the resonator admittance (weak coupling), and considering the lumped element situation, then if the shunt inductor has a value L and the coupling inductor has a value xL, where $x \gg 1$, then we may write

$$\frac{Z_e}{j\omega} = \frac{xL}{x-1}$$
$$\frac{Z_o}{j\omega} = \frac{xL}{x+1}. \tag{22}$$

Therefore

$$Z_e Z_o = \frac{x^2}{x^2+1}. \tag{23}$$

Hence

$$\sqrt{(Z_e Z_o)} = j\omega L. \tag{24}$$

Extending this to the distributed case, we may write

$$\sqrt{(Y_e Y_o)} = jY \cot \theta \tag{25}$$

where Y is the characteristic admittance of the combline resonator before the incorporation of the hybrid. Hence we have two simultaneous equations, (19) and (25), which can be solved numerically to give values of Z' and ϕ_1 for given Y_1, θ, ϕ, and Y.

As an example, the form of a third-degree, distributed hybrid channel filter is shown in Fig. 12. The end-loading capacitors on the combline resonators are realized by a combination of tuning screws and reduction of ground plane spacing over the ends of the resonators. The short circuits for the combline resonators are provided by plated through holes in contact with the upper and lower sections of the housing. Grounded walls are also placed between the end resonators and the through transmission lines to eliminate broadside coupling between line and resonator which would cause incorrect hybrid operation.

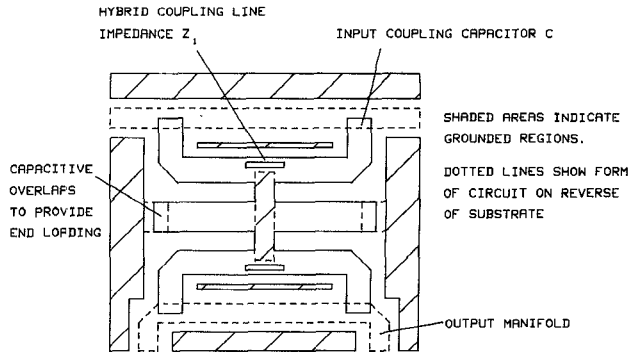

Fig. 12. Third-degree hybrid filter circuit based on the distributed hybrid of Fig. 11 and inverter coupled bandpass combline filters of the type shown in Fig. 10.

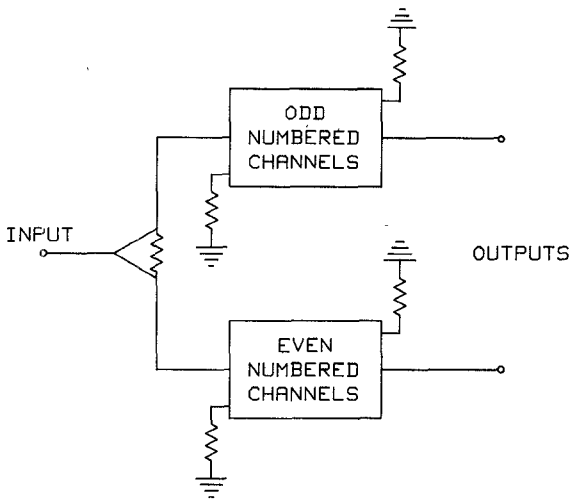

Fig. 13. Method of feeding recombining multiplexers.

V. Contiguous and Noncontiguous Multiplexers

The characteristics of the hybrid channel filter are such that the transmission between ports 1 and 2 on the manifold displays the same characteristics as the return loss of the individual channel filters. Hence for a lossless structure, the 3-dB points of the channel filter correspond to the 3-dB points of transmission along the manifold. If, however, the filters have a low finite Q (which is the case for printed circuit and lumped element filters with switching diodes incorporated), the situation becomes considerably worse. The lossy 3-dB points on transmission correspond to a point typically 9 dB down on transmission along the manifold.

The result of this is to make the signal reaching channels further down the manifold have a poor rolloff characteristic if the channels are made to be contiguous. Much-improved performance is achieved if the channel filters on any manifold are noncontiguous. The simplest configuration is to use two manifolds, one for the even-numbered channels and one for the odd-numbered channels. These two manifolds are then fed via a 3-dB Wilkinson splitter or 3-dB hybrid coupler as shown in Fig. 13. This is only possible as each multiplexer presents a broad-band input

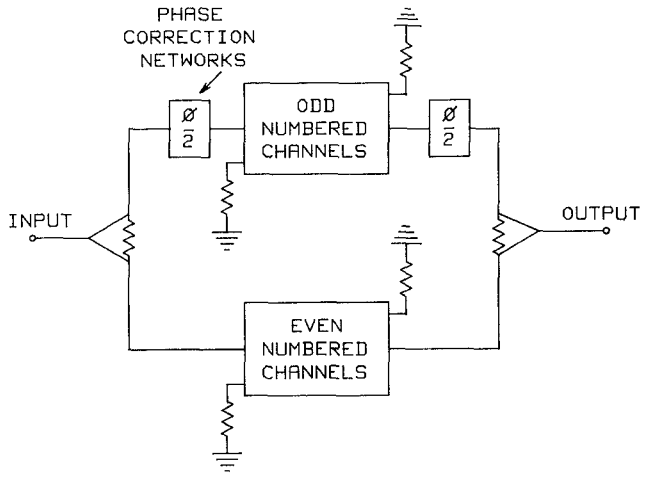

Fig. 14. Overall form of switched multiplexer.

match and hence does not introduce ripples in the passbands of the other multiplexer. Although the channels on each multiplexer recombine, the relative phase of transmission through each filter on a single manifold is not critical as there are no contiguous channels.

It is necessary, however, to connect the outputs of the two multiplexers in a manner such that outputs from two adjacent channels recombine with minimum amplitude variation. Let us consider the simple case of Fig. 14, where a Wilkinson power combiner is used. Suppose an arbitrary phase shift, ϕ, is incorporated to ensure the signals reaching the power combiner are in phase at crossover. Hence if the channel filters have a midband loss of X dB, the overall transmission loss through the device is

$$X + 6 \text{ dB} \tag{26}$$

assuming no contribution from the other channels. At the crossover point of each channel, two signals recombine in phase giving an overall transmission loss of Y dB, where Y is the band-edge loss of each channel. Hence, assuming the phase conditions can be met, the overall loss at crossover is the same as that in the midband of each channel provided the filters cross at their lossy 6-dB points. We require, however, that this loss level be constant for frequencies between these two points. This is difficult to calculate analytically as it requires an exact knowledge of the amplitude and phase response around the lossy 6-dB point of each filter.

Consider the outputs of two frequency translated low-pass prototype filters as shown in Fig. 15. The overall transfer function upon recombination may be expressed as

$$S_{12}(p) = \frac{1}{\sqrt{2}}\left[S'_{12}(p+j) + S'_{12}(p-j)\right] \tag{27}$$

where S'_{12} is the transfer function of a single low-pass filter. For an overall flat passband, we require

$$|S_{12}(j\omega)|^2 = \frac{1}{2\left(1+\epsilon^2 F_{2n}^2(\omega)\right)} \tag{28}$$

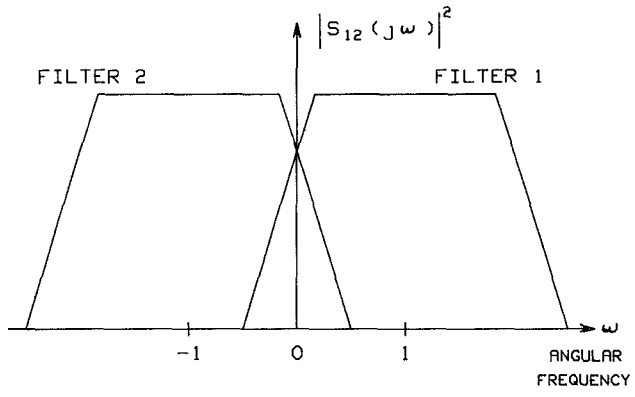

Fig. 15. Frequency translated low-pass prototypes.

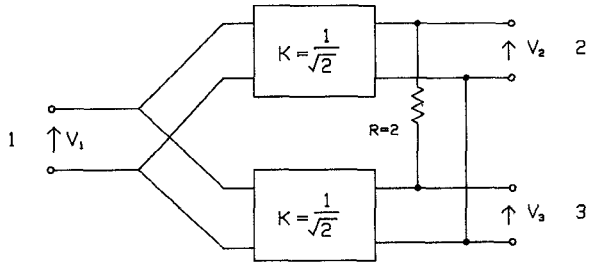

Fig. 16. Ideal power splitter/combiner.

where $F_{2n}^2(\omega)$ is a function of ω such that

$$|F_{2n}(\omega)| \leq 1 \qquad \text{for } -2 \leq \alpha\omega \leq 2 \tag{29}$$

where ϵ is a measure of the acceptable ripple level. Now each individual filter is based on a Chebyshev low-pass prototype, with a bandwidth scaling factor, α, such that $\alpha \approx 1$. Therefore

$$|S'_{12}(j\omega)|^2 = \frac{1}{1+\epsilon_1^2 C_n^2(\alpha\omega)} \tag{30}$$

where ϵ_1 and C_n are the measure of the prototype return loss level and a Chebyshev polynomial of degree n, respectively. It is fairly simple to derive $S'_{12}(p)$ from $|S'_{12}(j\omega)|^2$, but the expression of $|S_{12}(j\omega)|^2$ in the form of (28) is much more complex. This is made even more difficult when dissipation loss is included in (27) through (30).

A numerical approach was therefore pursued, as the calculation is relatively simple. For an ideal Wilkinson power combiner as shown in Fig. 16, the output voltage V_1 may be expressed as

$$V_1 = \frac{V_2 + V_3}{\sqrt{2}}. \tag{31}$$

As an example, two sixth-degree filters crossing over at 3 GHz with a lossless equiripple (0.1 dB0 bandwidth of 85 MHz were analyzed. The Q is 300, giving a -6 dB bandwidth of 100 MHz. These characteristics are taken as being representative of a typical switched multiplexer channel. Fig. 17 shows the resultant amplitude and group delay characteristics when a fixed frequency invariant phase shift of 100° is incorporated in one channel. The ampli-

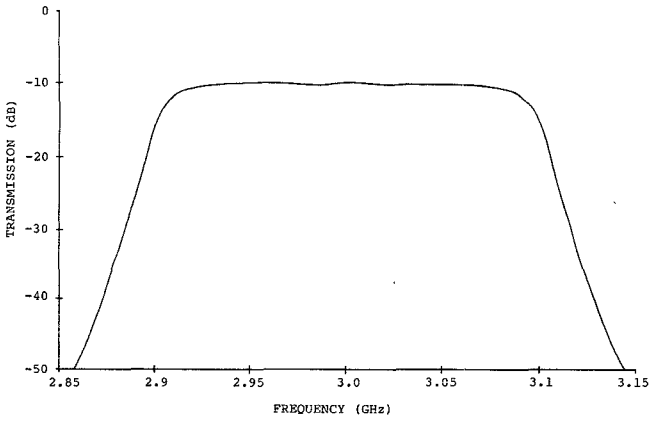

(a)

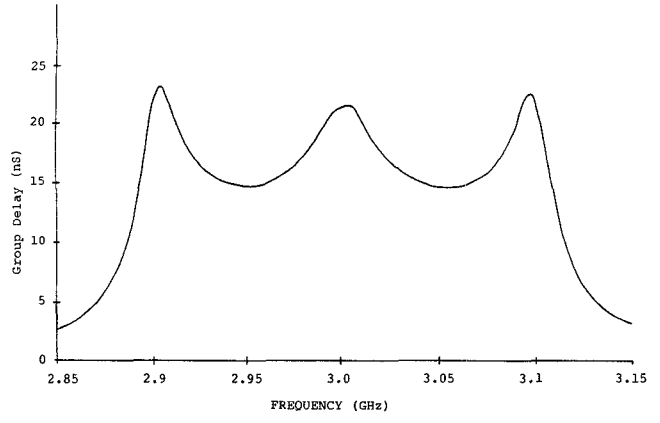

(b)

Fig. 17. (a) Amplitude response of two recombining multiplexer channels. (b) Group delay response of two channels.

tude characteristics are almost ideal but there exists a considerable group delay variation over the crossover region. Also, it is not practical to achieve a 100° relative phase shift at all crossovers in a complete switched multiplexer. The only readily achievable relative phase shifts are 0 or 180°. In the above example a 180° phase shift gives a phase error at crossover of 80°. By scaling the bandwidth of the channels so that the crossover points are less than -6 dB, the correct level of transmission can be achieved at the crossover point. Fig. 18 shows the resultant performance for the case discussed above.

The biggest difference from Fig. 17 is the much-improved group delay performance. This improved group delay is a result of two factors. Firstly, the channels are slightly wider and therefore cross over at a point of lower group delay. The main contribution, however, is a result of the deliberate phase error. At crossover, we may write V_2 and V_3 (the signals at the inputs of the combiner) as

$$V_2|_{\omega=\omega_0+\Delta\omega} = (V_0/\sqrt{2})(1-\alpha)\sin(\omega t + \phi_1 + \epsilon)$$

and

$$V_3|_{\omega=\omega_0+\Delta\omega} = (V_0/\sqrt{2})(1+\alpha)\sin(\omega t + \phi_2 + \epsilon). \quad (32)$$

Here, ω_0 is the crossover frequency, α is a measure of the rate of change of amplitude of each channel at crossover

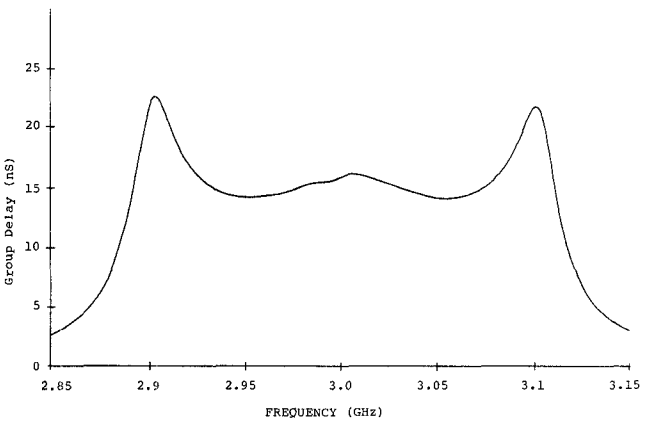

Fig. 18. Improved group delay response as a result of deliberate phase error.

(equal and opposite), and ϵ is a measure of the group delay of both channels at crossover:

$$T_g = \lim_{\Delta\omega \to 0} \frac{\epsilon}{\Delta\omega}. \quad (33)$$

Hence

$$V_1 = \frac{V_0}{2}\left[\sin\left(\omega t + \epsilon + \frac{\phi_1+\phi_2}{2}\right)\cos\left(\frac{\phi_2-\phi_1}{2}\right) + \alpha\cos\left(\omega t + \epsilon + \frac{\phi_1+\phi_2}{2}\right)\sin\left(\frac{\phi_2-\phi_1}{2}\right)\right]. \quad (34)$$

Let

$$a = \cos\left[\frac{\phi_2-\phi_1}{2}\right]$$

and

$$b = \alpha\sin\left[\frac{\phi_2-\phi_1}{2}\right].$$

Now

$$a\sin x + b\cos x = r\sin(x+k)$$

where

$$r = \sqrt{(a^2+b^2)} \text{ and } k = \tan^{-1}(b/a).$$

Hence

$$V_1 = \frac{V_0}{2}\left[\sqrt{(a^2+b^2)}\sin\left(\omega t + \epsilon + \frac{\phi_1+\phi_2}{2} + k\right)\right]. \quad (35)$$

Therefore at crossover, the group delay may be written as

$$T_g = \lim_{\Delta\omega \to 0} \frac{\epsilon + \tan^{-1}[\alpha\tan(\theta/2)]}{\Delta\omega} \quad (36)$$

where θ is the phase difference between the two channels $(\phi_2 - \phi_1)$.

Assuming α is positive, then for $\phi_1 > \phi_2$, the group delay at crossover is less than that for each individual channel, giving the result shown in Fig. 18.

Extending the above to a multichannel device is simple as all channels are normally designed using the same prototype. Although the example given is for one particular filter configuration, in practice it is usually possible to

achieve the desired performance with filters of any degree or Q factor by adjusting the return loss and bandwidth of the filter prototype.

The resulting switched multiplexer has good theoretical amplitude and phase characteristics, with the major disadvantage being the high insertion loss (approximately 10 dB). This is not a serious problem as gain is readily available for the IF bands where such devices are normally used.

VI. Experimental Results

Initial practical work was conducted on an eight-channel switched multiplexer with 100-MHz-wide channels operating in S-band. Each channel was based on a six-section, 0.1-dB-ripple Chebyshev prototype to give the performance shown in Fig. 18. These channels filters were realized in printed circuit combline form as discussed previously. By scaling the internal admittance level of each filter, every channel could be designed to be of the same physical length in order to make the input and output manifolds parallel.

Use was made of p-i-n switching diodes to effectively short out each of the four central resonators of the channel filters, using a total of eight diodes per channel. At first sight this may seem rather excessive, but it enables switching isolations of the order of 75–80 dB to be achieved. Due to the large number of diodes, only minimal forward bias is required for each diode ($\approx 200\ \mu$A), resulting in a total switch off current of approximately 2.5 mA per channel. The normal failure of p-i-n diodes is an open circuit and hence does not affect the on state of a channel. The large number of diodes enables typically 60-dB isolation specifications to be met even if some diodes fail. This considerably increases the MTBF of a complex switched multiplexer.

The required 180° phase difference between the even and odd channels was realized by a 90° meander line phase shifter [5] on one port of both the input and output power dividers. These circuits were realized using microstrip with $\epsilon_r = 10$, which allows easy realization of the meander line couplings.

Plots of switched multiplexer performance are shown in Fig. 19. These plots show the good amplitude and group delay performance of the unit as predicted by theory, with performance being limited by the accuracy of tuning of the device. Switching isolation was 75 dB except in channel 3, where a diode was faulty, indicating the value of diode redundancy. Overall switching speed (50 percent TTL to within 10 dB of final rejection or 3 dB of final passband) was measured to be approximately 40 nS. Again, this parameter was improved by the presence of diodes on all the central resonators of each channel, which allows RF energy to be "quenched" rapidly. The use of hybrid channel filters enables the input and output match to be preserved even when channels are switched off, this parameter being important with respect to intermodulation performance particularly if the device is preceded or followed by a mixer.

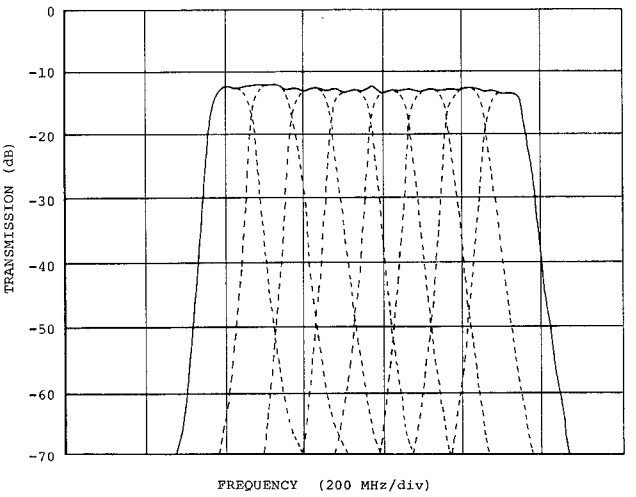

(a)

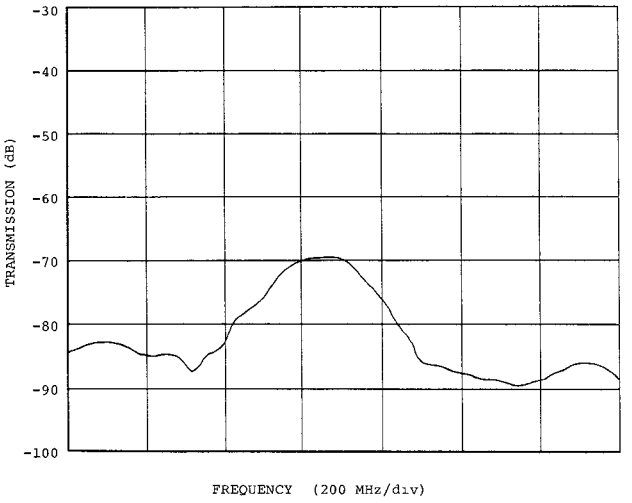

(b)

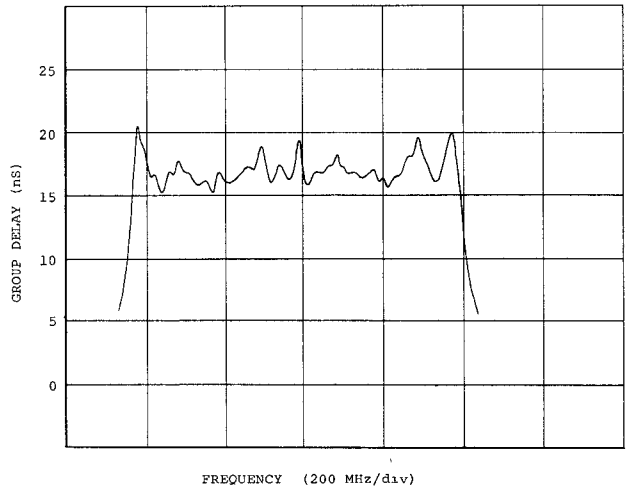

(c)

Fig. 19. Measured performance of eight-channel switched multiplexer. (a) Each channel switched on individually with plot of all channels on at the same time superimposed. (b) Response showing all channels switched off. (c) Group delay—all channels on.

VII. Conclusions

The use of four-port hybrid filters based on integral 3-dB hybrid couplers allows multiplexers having large numbers of narrow channels to be easily realized, particularly in printed circuit form. As such multiplexers are matched in both passband and stopband, they may readily be fed from simple power splitting networks. This enables a recombining multiplexer having low amplitude ripple to be realized. Furthermore, by introducing the correct phase in one path of such a multiplexer, very low group delay ripple results. Multiple diode switching circuits enable switched multiplexers to be constructed with very low power dissipation (less than 20 mW per channel) and high mean time between failure.

Practical results on switched multiplexers designed using the method presented confirm the validity of the design technique. The devices are relatively simple to build and align due to the elimination of interactions between channels. The use of accurate photolithographic methods eliminates much of the tuning required in such a multiplexer and makes the construction of devices having very large numbers of channels practical.

Acknowledgment

The author would like to thank Prof. J. D. Rhodes for his help and advice during the course of this work, K. W. Ferguson for the continued development of the techniques described in this paper, and A. Marshall for the preparation of the diagrams.

References

[1] W. A. Edson and J. Wakabayashi, "Input manifolds for microwave channelizing filters," *IEEE Trans. Microwave Theory Tech.*, vol. MTT-18, pp. 270–276, May 1970.

[2] J. D. Rhodes, *Theory of Electrical Filters*. New York: Wiley, 1976, ch. 4, pp. 127–128.

[3] G. L. Matthaei, "Comb-line band-pass filters of narrow or moderate bandwidth," *Microwave J.*, vol. 6, pp. 82–91, Aug. 1963.

[4] W. J. Getsinger, "Coupled rectangular bars between parallel plates," *IRE Trans. Microwave Theory Tech.*, vol. MTT-10, pp. 65–72, Jan. 1962.

[5] B. M. Schiffman, "A new class of broadband microwave 90 degree phase shifters," *IRE Trans. Microwave Theory Tech.*, vol. MTT-6, pp. 232–237, Apr. 1968.

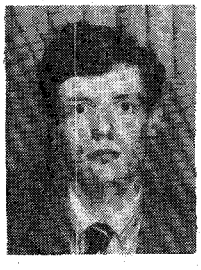

Christopher I. Mobbs (M'87) was born in Leeds, England, in 1962. He received the B.Sc. (Hons.) and Ph.D. degrees from the University of Leeds in 1982 and 1986, respectively.

Since 1982 he has worked for Filtronic Components Ltd., Shipley, England, involved in the development of a variety of new filter and multiplexer designs. His current work is in the area of filter related subsystems including switched multiplexers and high-speed direct frequency synthesizers.